An acoustic FM–CW radar for atmospheric sounding

G. E. Perona

Istituto di Elettronica, Politecnico di Torino, Torino, Italy

R. U. Pisani

Istituto Elettrotecnico Nazionale, "Galileo Ferraris," Torino, Italy
(Received 11 August 1977; revised 4 October 1978)

A prototype FM–CW radar for atmospheric sounding and some of its applications are described. The prototype generates a signal whose frequency increases linearly from 1830 to 2160 Hz during a time interval of 10 s, the excitation being at intervals of 20 s. The principle of operation is based on the fact that received echos reflected from inhomogeneities at height h, will have a frequency lower by an increment of (df/dt) $(2h/c)$ than that currently being transmitted. Typical data taken with the prototype are compared with analogous data obtained with a pulsed SODAR.

PACS numbers: 43.28.Tc, 43.28.Fp

INTRODUCTION

In recent years, many acoustic systems have been developed for the sounding of the lower atmosphere. (See, e.g., Refs. 1–4.)

These instruments have been used to analyze the atmospheric turbulence, and wind and temperature structure. The principle of operation is straightforward: acoustic pulses, a few tens of milliseconds long, are sent vertically by an acoustic antenna; the acoustic power, backscattered or sidescattered, is received by the same or by other acoustic antennas. This approach has some limitations due to many causes: first of all, returns from fixed obstacles in the neighborhood of the transmitting antenna may confuse the useful echoes of atmospheric origin from low-height levels; secondly, the height resolution is limited by the length of the transmitted pulse; thirdly, fast changing structures in the atmosphere may not be followed in detail, since the pulses are transmitted necessarily at many seconds intervals. These or similar problems are encountered also by electromagnetic radars; in this case, such problems have been partly overcome by the use of frequency-modulated, continuous-waves radars (FM–CW radar) mainly at the cost of an increase in the complexity of the system. Such electromagnetic radars operate on the following principle (see, e.g., Refs. 5 and 6): the transmitted frequency changes continuously, during a time interval Δt, from f_0 to $f_0 + \Delta f$: the signal received by a second antenna is mixed with the transmitted signal and, then, the beat frequency is revealed: the beat frequency is proportional to the time delay of the reflected signal, that is to the distance of the reflecting target. With this radar, the distance resolution is of the order of $c/\Delta f$ where c is the light velocity, while the equivalent bandwidth is $2/\Delta t$.

In this paper an acoustic FM–CW radar for atmospheric studies is described. The system is a prototype that has been assembled with laboratory equipment to show the feasibility of this technique and to roughly estimate its performance. A partial comparison with results obtained with a traditional SODAR is also presented, just for demonstration purposes.

I. PRINCIPLE OF OPERATION

The acoustic FM–CW radar is described in Fig. 1: the trigger pulse from the trigger generator starts a ramp that, in turn, feeds a voltage-controlled oscillator (VCO). The output of the VCO is a frequency-varying signal from $f_0 = 1830$ Hz at the beginning of the ramp, to $f_0 + \Delta f = 2160$ Hz at its end. The signal amplitude is zero at the end of the ramp. The total length of the ramp, Δt, is 10 s. The repetition rate of the trigger pulses is $2\Delta t$. In this way, each 10-s transmission is followed by a 10-s intermission, introduced to have enough time to process the return signal with the system in use.

The output of the VCO is amplified; the acoustic signal is then radiated upward from a 1.20-m paraboloid (T). The backscattered signal is received by a second 1.20-m paraboloid (R). In order to reduce the acoustic noise, the signal is filtered with a $\frac{1}{3}$-octave bandwidth.
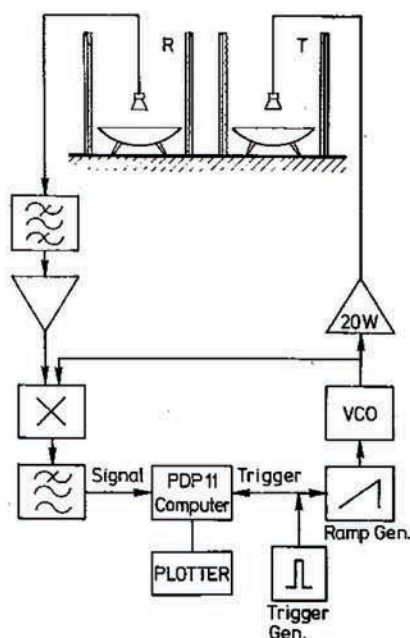

FIG. 1. Block diagram of the FM–CW acoustic radar.

After amplification, the signal is multiplied with the transmitted signal. As a consequence of this heterodyning procedure, the multiplier output contains two sidebands, the lower one just above zero frequency and the other one at about twice the transmitted frequency. Such an output is low-pass filtered with a 150 Hz cutoff frequency. In the analog processing of the signal, laboratory instrumentation having dynamic range larger than 70 dB has been used, with the only exception of the multiplier that has a dynamic range not much larger than 50 dB.

Finally, a minicomputer samples the low-frequency signal, performs its Fourier transform, and then presents its power spectrum on a video display.

The principle of operation is described in Fig. 2. The transmitted frequency as a function of time is represented by the line labelled $h = 0$ m. The signal backscattered by a target at a height h reaches the receiving antenna after the time $2h/c_0$, where the sound velocity c_0 is assumed to be equal to 343 m s^{-1} in what follows. Consequently, the frequency shift df between the signal transmitted and received is equal to $(\Delta f/\Delta t) 2h/c_0$. Each oblique, light line in Fig. 2 represents schematically the return signal from different height levels. For convenience in the data comparison with the results of our pulsed SODAR, the observation height has been limited to levels below 686 m that corresponds to $df = 132$ Hz (see Fig. 2). In this way, in the analog signal at the output of the low-pass filter in Fig. 1, the amplitude of each spectral line at frequency df, represents the echo obtained from the height $h = df \cdot c_0 \cdot \Delta t/(2 \cdot \Delta f)$. The details of the Fourier analysis performed on the signal are the following: the signal is digitally converted at a sampling frequency of 512 Hz with a 12-bit A/D converter; the data have been collected within a 9-s time window, starting from the trigger pulse. However, in order to use our FFT algorithm, only 4096 data points have been analyzed, corresponding to an 8-s effective time window; the first 512 data points collected have not been used, avoiding in this way problems connected with
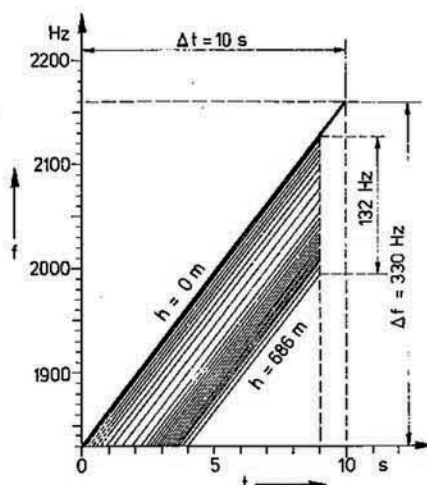
the initial transients. Care has been taken to evaluate the effects of the leakage due to the finite size of the time window, which has not been smoothed by any tapering procedure. In the present case, a sinusoidal signal 8 s long, at approximately 4 Hz would give a power spectrum more than 25 dB below the main line at about 5 Hz.

In the power spectrum of the low-frequency signal represented by the video display, the frequency scale may be uniquely and linearly related to height: the level of each spectral line is proportional to the power reflected by the corresponding height level. As it appears from Fig. 2, the signal backscattered from higher levels is received for a shorter time interval within the 8-s time window. Consequently each spectral line for $df > 33$ Hz has been multiplied by the correction factor $(\Delta f - 66)/(\Delta f - 33 - df)$. It is to be noted that the frequency resolution of the spectrum is $1/8$ s^{-1}, corresponding to an equivalent height resolution of 0.65 m. Of course, this value is not realistic since the vertical stochastic motion of the air turbulence produces Doppler broadening of the echo, significantly reducing the equivalent height resolution (e.g., a 0.1 m/s vertical velocity would produce a Doppler shift of about 1.2 Hz for a carrier frequency of 2000 Hz, thus producing a range error of about 6 m). For this reason, a running average over ten spectral lines has been performed on the data presented. However, the distance resolution is equal to the theoretical one for fixed nearby reflecting obstacles: this fact could be exploited to eliminate the low-level echoes from the "clutter."

Furthermore, it should be realized that the echo level received from a fixed height does not usually remain constant for the sounding period Δt: the FM-CW SODAR may make it possible, through a data analysis different from the one described in this paper, to continuously follow the time history of the turbulence at the different levels.

Of course, one of the problems encountered in the realization of the system is the strong direct signal received by the receiver antenna R. Indeed, the sound pressure level measured at 1 m above the antenna T is 120 dB at 2000 Hz. Even taking into account the antenna separation (3 m) and the antenna directivity, the direct signal from T to R would be extremely large in comparison with the backscattered signal. For this reason and to reduce the traffic noise in the receiver, acoustic shielding of the antennas has been provided. The shields are 3 m high and are inside-coated with resonant absorbing plates. In this way, the direct sound pressure level measured with an omnidirectional microphone 30 cm above the focus of the receiver is 60 dB. Care has been taken to reduce diffraction effects due to the edges of the shields by coating the edges with glass wool. Evidently, the screens also reduce the side lobe level, and therefore improve the performance of the system in reducing both the annoyance and the level of fixed echoes. The traffic noise, measured inside the R screen with the same microphone, in the octave band centered at 2000 Hz, is 20 dB SPL, which corresponds to a 15.3 dB SPL in the $\frac{1}{3}$-octave band used in the experiment.
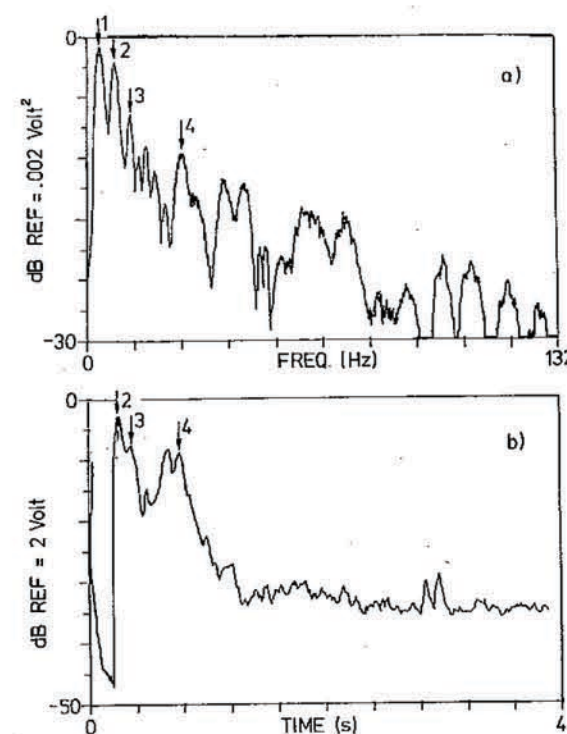
FIG. 3. Spectrum of the signal received by the FM-CW acoustic radar at h. 6.20 in the morning (a) and SODAR-received pressure level averaged over 10 successive pulses at h. 6.15. In the two figures, frequency and time scale correspond to the same height levels (686 m → 132 Hz → 4 s).

Furthermore, the use of a frequency-modulated signal requires a flat frequency response characteristic of the whole system. In order to check the response curve, the input–output transfer curve has been computed by feeding white noise in the transmitting chain and measuring the output of the receiving chain. The transfer function, computed by the PDP 11, appears to be sufficiently flat in the frequency range of interest: in any case, such a function could be used to introduce correction factors in the results.

In order to evaluate the performance of the system with respect to the background noise, a series of records have been taken with the transmitter off during daytime hours, when the city noise was at its maximum. The output spectrum in the frequency of interest is flat and equal to $33 \cdot 10^{-7}$ V^2. In this way, the signal-to-noise ratio of the data to be presented may be easily evaluated. Indeed, the two measurements performed with the omnidirectional microphone, of the direct signal and of the noise inside the receiving screen, imply a dynamic range of 44.7 dB. This quantity compares quite well with the FM-CW results: the maximum signal (direct signal) measured by the FM-CW equipment is approximately 3 dB below 0.2 V^2 reference level as it will appear later on (Fig. 5); consequently the dynamic range in the performed measurements comes out to be at least of the order of 44.8 dB, as expected from the omnidirectional microphone measurements.

A noteworthy improvement in the dynamic range (of the order of 8 dB) may be reached during the hours of minimum traffic noise.

It is to be noted that even a larger dynamic range could be needed to study higher atmospheric levels; in this case, the acoustic noise inside the screen should be drastically decreased and, at the same time, a filtering-out of the direct signal by a band-reject filter tuned to the transmitted frequency could be needed.

II. EXPERIMENTAL DATA

A series of acoustic soundings of the atmosphere in different meteorological situations have been performed. Figure 3(a) shows the spectrum obtained on June 21, 1977 at 6.20 solar time in the morning, in Turin (Italy), during a clear day. A 4-Hz high-pass filter has been inserted in order to eliminate, for convenience in the representation, the first strong spectral lines, which will be presented later in other expanded figures. It is to be noted that, in the present case as a consequence of the low traffic noise at these early hours in the morning, the noise level was roughly 8 dB below the noise level measured during daytime hours, as discussed in the previous section.

In order to compare these data with the results of a pulsed SODAR, Fig. 3(b) presents an average of 10 successive soundings at 2000 Hz, of 50-ms pulses repeated 5 s apart, taken 5 min before the FM-CW sounding. The receiver is not operating for the first 250 ms after the start of the transmitted pulse.

Some correspondences between structures in the two figures are pinpointed by arrows. The strong echo (arrow 1) in Fig. 3(a) cannot appear in Fig. 3(b), due to the delay in the starting time of the receiver record. It should be remembered that the FM-CW radar gives echoes averaged over many seconds and over a very short height range at any given height level, while the
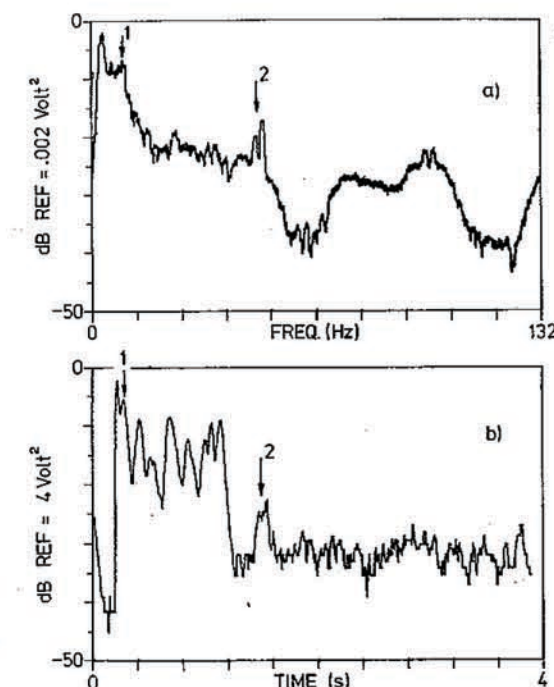
FIG. 4. Spectrum of the signal received by the FM-CW acoustic radar (a) and the SODAR-received pressure level squared of a single pulse 10 s afterwards.
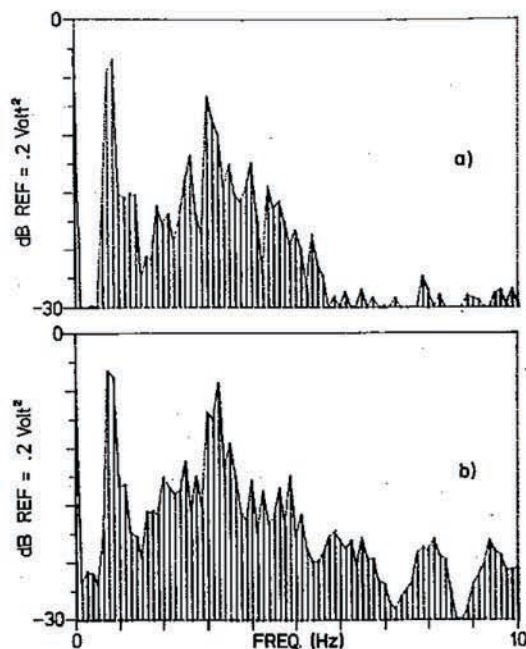
FIG. 2. Scheme of operation: frequency transmission versus time. The shaded region represents the received signal effectively analyzed.

J. Acoust. Soc. Am., Vol. 65, No. 5, May 1979

G. E. Perona and R. U. Pisani: Acoustic FM-CW radar

J. Acoust. Soc. Am., Vol. 65, No. 5, May 1979

G. E. Perona and R. U. Pisani: Acoustic FM-CW radar

FIG. 5. Expanded FM-CW spectra in the low-frequency range 0–10 Hz corresponding to a height range of 52 m.

FIG. 6, Correlation between transmitter input and receiver output obtained feeding white noise in the transmitter.

SODAR represents the atmospheric situation in an extremely short time interval, averaged over a height range of the order of the pulse length. As a consequence of these fundamental differences between the two sounding procedures, no detailed correspondences between the records is expected.

In order to better characterize the comparison between the two systems, Fig. 4 shows an FM-CW spectrum and the SODAR data, obtained by a single pulse, transmitted 10 s after the FM-CW sweep (h 7.05 solartime of the 21/6/77). In this case, the effects of the integration implicit in the FM-CW system is even more evident. Note that in this figure, the SODAR signal [Fig. 4(b)] has been squared, and consequently, the reference level is different from that in Fig. 3(b).

Figure 5 shows two expanded FM-cw spectra in the low-frequency range 0–10 Hz, which corresponds to a height range of 52 m. In this case, no 4-Hz high-pass filter has been inserted and the 10-line average procedure has been omitted. It is quite evident that the presence of the fixed peak is due to a screen-diffracted ray at 0.75 Hz and a second fixed peak at about 3.3 Hz is due to reflection from a nearby wall. Such spurious echoes can be easily detected and eventually removed. It is to be noted that the high variability in the spectrum structures of the two drawings, is due to atmospheric turbulence. This fact shows the possibility of using the FM-CW radar in a slightly more sophisticated version to study extremely low height levels.

Figure 6 shows a correlation between transmitter input and receiver output obtained feeding white noise in the transmitter: the peak at $\tau = 0.022$ s corresponds to
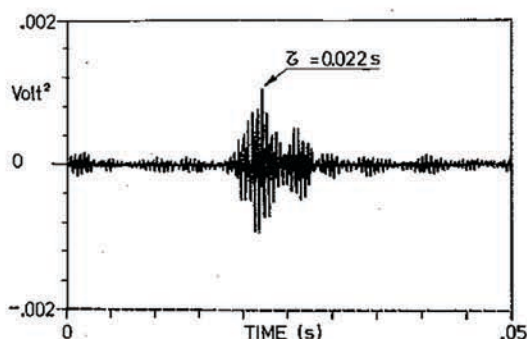
the diffracted ray seen at 0.75 Hz in the previous figure. The direct ray through the walls of the screens does not appear clearly in the figure since its level is much lower than the diffracted ray, as a consequence of the very high reduction index of the structures.

III. CONCLUSIONS

The first experiments performed with the FM-CW acoustic radar have shown the feasibility of such a system and its ability to perform very-low height sounding of the atmosphere. Of course, the hardware is much more sophisticated than in the pulsed radar (SODAR). However, the possibility of using low-cost microcomputer and fast Fourier transform hardware, could permit the implementation of the system in a compact form.

Such a system may be particularly suited to operate in a noisy environment with low-power output for studies of the surface layer.

[1] L. G. McAllister, "Acoustic sounding of the lower troposphere," J. Atmos. Terr. Phys. 30, 1439–40 (1968).
[2] C. G. Little, "Acoustic methods for the remote probing of the lower atmosphere," Proc. IEEE 57, 571–578 (1969).
[3] D. W. Thomson, "Applications and limitations of Doppler acoustic sounders for planetary boundary layer studies," Summary Report 3rd Workshop in Atmospheric Acoustics, Toronto, 1975.
[4] M. Chong, "Measures des profils de vent par sodar-doppler," CRPE note technique, 22 (1976).
[5] J. H. Richter, "High resolution tropospheric radar sounding," Radio Sci. 4, 1261–1268 (1969).
[6] J. H. Davies and V. Ward, "An Airborne FM-CW Radar for Monitoring Small Scale Atmospheric Layering Effects," Atmosphere 12, 512–516 (1974).